Fatigue in continuous fibre reinforced thermoplastic composites

Sergio Díaz Cardona

Trabajo de grado para optar al título de Ingeniero Mecánico

Director

Octavio Andrés González Estrada, PhD.

Ingeniero Mecánico

Universidad Industrial de Santander

Facultad de Ingeniería Físico-Mecánicas

Escuela de Ingeniería Mecánica

Bucaramanga

2018

Acknowledgements

First of all, I want to thank my family for always being present and giving me all their support and love, my mother Regina Maria, my Father Juan Guillermo, my brother Santiago and my aunt Estella. This achievement is also yours.

I would also like to show me gratitude to the Mechanical Engineering Department of the Industrial University of Santander for their great academic and human work, and the GIEMA research group for their support.

Special thanks to the Electron Microscopy laboratory at Universidad Industrial de Santander, located in Guatiguará, for their cooperation in the Fractographic analysis.

Sergio Díaz Cardona

Contents

Tables

Figures

Resumen

TÍTULO: CARACTERIZACIÓN A FATIGA UNIÁXIAL EN MATERIALES COMPUESTOS IMPRESOS EN 3D REFORZADOS MEDIANTE FIBRAS CONTINUAS [*]

AUTORES: SERGIO DÍAZ CARDONA [**]

PALABRAS CLAVES: Materiales termoplásticos compuestos reforzados con fibras continuas (CFRTPC), modelado por deposición fundida (FDM), manufactura aditiva (AM), Fatiga en termoplásticos.

DESCRIPCIÓN: Las tecnologías de manufactura aditiva han sido probadas con éxito en diferentes aplicaciones. La técnica de modelado por deposición fundida (FDM), es la técnica más utilizada para fabricar piezas hechas en materiales termoplásticos debido a su bajo costo de manufactura y bajo porcentaje de material desperdiciado y ha sido implementada mediante impresoras 3D.

Las piezas de material termoplástico manufacturadas mediante FDM presentan unas propiedades mecánicas las cuales son insuficientes para manufacturar piezas funcionales. Debido a este problema nuevas tecnologías fueron creadas con el propósito de reforzar los filamentos termoplásticos mediante fibras cortas, largas o continuas en los últimos años. Las impresoras 3D que manufacturan materiales termoplásticos compuestos reforzados con fibras continuas (CFRTPC) están llevando esta tecnología a un nuevo nivel en términos de eficiencia de producción, bajo desperdicio de material y de óptimas propiedades mecánicas. Por este motivo, se hace necesario el estudio del comportamiento mecánico bajo cargas estáticas y dinámicas de las piezas manufacturadas para determinar si estas cumplen con las propiedades mecánicas necesarias para ser consideradas piezas funcionales. El propósito de este trabajo es el de presentar el estado del arte actual de los CFRTPC y el de caracterizar el comportamiento bajo cargas de fatiga uniaxial de los materiales compuestos impresos en matriz en nylon reforzados por fibras de vidrio, fibras de carbono y fibras de kevlar

[*] Trabajo de grado

[**] Facultad de Ingenierías Físico-Mecánicas. Escuela de ingeniería Mecánica. Director: Ing. Octavio Andrés González Estrada

Abstract

TITLE: FATIGUE IN CONTINUOS FIBRE REINFORCED THERMOPLASTIC COMPOSITES.[*]

AUTHORS: SERGIO DIAZ CARDONA[**]

KEYWORDS: Continuous fibre reinforced thermoplastic composites (CFRTPCs), fused deposition modeling (FDM), additive manufacturing (AM), Fatigue in thermoplastics.

DESCRIPTION: Additive manufacturing (AM) technologies have been applied with success in many applications. Fused deposition modeling (FDM), is the most widely used AM technique for fabricating thermoplastic pieces due of its low manufacturing cost and and low percentage of wasted material and has been implemented using 3D printers.

The pieces of thermoplastic material manufactured by FDM have mechanical properties that are not optimal for the production of functional and load-bearing parts. Due to this problem, new technologies were created with the purpose of reinforcing the thermoplastic filaments with short, long or continuous fibers in recent years. 3D printers that manufacture composite thermoplastic materials reinforced with continuous fibers (CFRTPC) are taking this technology to a new level in terms of production efficiency, low material waste and optimal mechanical properties. For this reason, it is necessary to study the mechanical behavior under the static and dynamic loads of the manufactured pieces, to determine if they satisfice the mechanical properties condition necessary to be considered as functional pieces. The purpose of this work is to present the actual state of the art of the CFRTPC and to characterize the behavior under uniaxial fatigue loads of composite materials printed on matrix in nylon reinforced by glass fibers, carbon fibers and fibers from Kevlar.

[*] Degree work

[**] Faculty of Physical-Mechanical Engineering. School of Mechanical Engineering. Director: Ing. Octavio Andrés González Estrada

Introduction

Additive manufacturing (AM) is a process of joining materials, layer upon layer, in order to create objects from 3D model data ("Standard terminology for additive manufacturing technologies," 2012). With AM technologies it is possible to achieve the construction of a large range of prototypes or functional pieces with geometries which are difficult to be manufactured by the conventional fabrication methods (Alimardani, Toyserkani, & Huissoon, 2007; Yakovlev, Trunova, Grevey, Pilloz, & Smurov, 2005). In comparison with conventional methods, AM is more effective since it can reduce the design-manufacturing cycle and thus, diminish the production cost and increase the competitiveness (Hague, Campbell, & Dickens, 2003),(Der Klift et al., 2016).

Among the AM techniques, fused deposition modelling (FDM) is the most widely used methods, because of its low cost and the minimal material wasted (Dudek, 2013). Currently, the majority of the feedstocks used in FDM are thermoplastic filaments as, polycarbonate (PC), polylactide (PLA), and polyamide (PA) (Ning, Cong, Qiu, Wei, & Wang, 2015).

The thermoplastic parts made by FDM suffer from the lack of strength as the fully functional and load-bearing parts (Zhong, Li, Zhang, Song, & Li, 2001). Due to this restriction, researchers developed new technologies to reinforce with fibres the thermoplastic filaments (Ning et al., 2015; Zhong et al., 2001), in order to improve the mechanical properties of the produced parts. Hence, FDM provides a possibility for manufacturing complex functional and structural parts with fibre reinforced thermoplastic composites (FRTPCs).

Nowadays, thermoplastic matrix fibre reinforced composites are widely used in aerospace, medical, and automobile industry and electronics applications (Ahn, Montero, Odell, Roundy, & Wright, 2002; Leigh, Bradley, Purssell, Billson, & Hutchins, 2012). In the field of the FRTPC several improvements have been made, continuous fibre reinforced thermoplastic composites (CFRTPC) printers are taking this technology to a whole new level in terms of efficient production and mechanical properties (Der Klift et al., 2016).

Melenka et al. [16] evaluated the elastic properties of the CFRTPC printed on the MarkOne printer, and predicted the elastic properties using an Average Stiffness (VAS) method. The specimens were printed varying the volume fraction of the fibres. The results showed that an increase in the volume fraction of fibre reinforcement results in an increase in stiffness and ultimate strength of the specimen.

Ning et al. [9] in their research with FRTPCs, tested the effect of adding carbon fibre with different content and length to improve the mechanical properties of different parts fabricated by FDM. Effects on the tensile properties (tensile strength, Young's modulus, toughness, yield strength and ductility) were experimentally investigated. They found from the tests an increase in the tensile strength and in Young's modulus, but a decrease in the toughness and ductility of the specimens tested.

Yang et al. (Yang, Tian, Liu, Cao, & Li, 2017) studied the mechanism of 3D printers for CFRTPC. They performed several mechanical tests such as three-point bending, tensile and interlaminar shear in order to characterize the CFRTPC mechanical properties. The results showed an improvement of the 10 wt% CCF/ABS specimens in the flexural and tensile strength with 127

MPa and 147 Mpa respectively, which is greater than the ABS specimens and close to the CCF/ABS (injection moulding) with the same fibre content.

Van der Klift et al. (Der Klift et al., 2016) evaluated the capabilities of the Mark One 3D printer in CFRTPC with carbon fibres. They printed several CFRTPC specimens with three different configurations and made a tensile test in the longitudinal direction to overview the mechanical properties of the specimen. The results showed an improvement in the tensile properties.

Also, they found that the behaviour of the CFRTPC is not in complete agreement with the traditional mixing rules for composites due to the delamination and the cavities formation. The results showed as well that the discontinuities of the fibres produced a premature failure in the areas where the fibres were absent.

Another study of CFRTPC was investigated by Mori et al. (Mori, Maeno, & Nakagawa, 2014) using a RepRap printer. However, they did not determine the elastic properties of the CFRTPC.

Tian et al. (Tian, Hou, Li, & Lu, 2016) introduced a mechanism for FDM of CFRTPC to produce pieces for aerospace applications and analysed the influence of the process parameters, such as, the content of the fibre and its orientation, on the mechanical properties of CFRTPC specimens.

Nanya Li et al. (Li, Li, & Liu, 2016) performed a study with CFRTPC polylactic acid (PLA) printed by the rapid prototyping approach to 3D printing. The PLA suffered a modification with a methylene chloride agent to increment the interfacial strength between carbon fibre and resin.

The results of the mechanical tests performed showed an increment of 13,8% and 164% in the tensile and flexural strenght, respectively, of modified carbon fibre reinforced composites compared to original carbon fibre reinforced specimens. Also, they found an increment of the

storage modulus for about 166% and 351% of the modified carbon fibre reinforced composites compared to PLA and original fibre reinforced specimens, respectively.

In the last years, the fatigue behaviour of plastics has called researchers attention due to the application possibilities in aerospace, automotive and biomedical industries. Afrose et al. [19] examined the fatigue behaviour of (PLA) parts processed by FDM. They performed fatigue tests in concordance with ASTM D638, for different build orientations and percentage nominal values of the ultimate tensile stress.

Specimens manufactured in X-direction showed the longest lifetime for stresses greater than 15 MPa. Around 10e4 load cycles, an important reduction in the stress can be seen in all directions. The S-N curves for the X and Y directions converge after 3000 load cycles and after 10e5 load cycles, almost coincide. No direction can be recognized after around 10e6 load cycles.

The results for the tension-tension fatigue tests demonstrated that +45/-45° specimens had the longest fatigue life for each stress level, followed by the 0,45 and 90° orientation. Furthermore, the results showed anisotropic behaviour on the raster orientations; a different number of cycles to failure for the raster orientations and similar failure modes as those seen in static tests.

Ziemian et al. (Ziemian, Okwara, & Ziemian, 2015) performed a tensile-fatigue test on layered acrylonitrile butadiene styrene (ABS) components fabricated by FDM, in accordance with ASTM D638 standard. This test was executed for different raster orientations and ultimate tensile stresses.

The results showed dependence to various parameters such as stress amplitude, manufacturing defects present in the specimens, temperature, frequency and environment. The specimens

manufactured with fibres orientation in 45° presented higher fatigue life and a higher storage modulus compared to parts build in X and Y configuration for the same applied loads.

Many factors, such as processing conditions, fibre length and orientation, properties and configuration of the composite matrix, interfacial properties and testing conditions, have an important effect in the fatigue behaviour of discontinuous fibre reinforced polymer matrix composites.

Goel et al. (Goel, Chawla, Vaidya, Chawla, & Koopman, 2009) studied the fatigue behaviour of long fibre reinforced thermoplastic composites (polypropylene/20 volume % E-glass fibre) in terms of stress – number of cycles to failure curves.

After testing specimens along the longitudinal and transversal direction, they established that the specimens tried along longitudinal direction performed better under the same fatigue load conditions. They additionally noticed that fatigue life diminished with increment in frequency. They associated this response with the hysteretic heating that takes place at high frequencies and, furthermore, because of the poor thermal conductivity properties of the thermoplastic matrix.

Because long fibre reinforced thermoplastics have higher thermal conductivity than unreinforced thermoplastics and, subsequently, quicker heat dissipation to the surroundings occur, they demonstrated a lower temperature rise contrasted with the unreinforced ones.

To predict the fatigue life in fibre reinforced thermoplastics is a difficult task. They are anisotropic and show a variety of damage mechanisms. There are a considerable number of empirical formulas in the literature to predict fatigue of composites (Brunbauer & Pinter, 2015), however, they are constrained to particular loading restrictions and environment. The fatigue damage

process has both creep and fatigue effect. Creep tends to relax the strains and increase the fatigue life of the composite part. (Bhuiyan & Fertig, 2017)

The importance of the creep strain accumulation during the fatigue is very important. The accumulated creep strain relaxes local stresses and, subsequently, substantially modifies the predicted fatigue life. Regardless of this well-known phenomenon, coupling of physics-based methodologies for durability prediction of fibre reinforced thermoplastics combining fatigue with creep has been implemented.

Fertig et al. (Kuhn & Fertig III, 2016) have proposed a physics-based fatigue methodology based on the kinetic theory of fracture (KTF), which have been successfully implemented to predict fatigue and creep of composite structures.

KTF models the damage mechanism as a thermally activated process and uses the physics of the matrix material to keep track of the damage accumulated in the composite. The steps of the process are: (i). link volume-averaged composite stresses and strains to volume-averaged matrix stresses and strains, (ii). evaluate the damage in the matrix due to fatigue using KTF, (iii). Analyse and compare the microscopic bond breaking and the macroscopic behaviour of the structure (Bhuiyan & Fertig, 2017).

Several fatigue models have been used to predict the fatigue life of composite materials. The Basquin's model is used because their accuracy and simplicity in the fatigue tests of fibre reinforced composites specimens (Basquin, n.d.).

1 Problem statement

1.1 Identification of the problem

The majority of filaments used as raw material in FDM technology are thermoplastics, due to this, the pieces obtained lack the necessary resistance to be functional pieces, limiting their applications to rapid prototyping (Tekinalp et al., 2014). Due to this, it was necessary to find a new method that would increase the strength of the parts manufactured by FDM.

One of the methods used was to add short fibres of reinforcing materials to thermoplastic matrices, such as carbon fibres. The short reinforcing fibres are used to support the applied load, while the thermoplastic matrix is used to bond and protect the fibres and transfer the load to the reinforcing fibres.

The pieces reinforced by fibres, exhibit better mechanical properties such as tensile and bending strength, make them available for being functional pieces (Ning, Cong, Qiu, Wei, & Wang, 2015). The School of Mechanical Engineering of the Industrial University of Santander, recently acquired a 3D printer that allows to print pieces reinforced by continuous fibres, this is the MarkOne made by MarkForged.

This printer reinforces 3D printed parts with kevlar, glass and carbon fibres. It also allows to choose the deposition angle of the fibres and the filling pattern of the matrix.

In comparison to conventional reinforcement methods that use short fibres, the MarkOne printer uses continuous fibres which allow producing specimens with better mechanical properties in a short production time and with less waste of material.

This makes the MarkOne printer a novel manufacturing technology that takes the production of reinforced composites to a new level for implementation as functional parts.

To establish the applications of the pieces obtained, it is necessary to carry out the characterization of their mechanical properties and compare them with the respective design specifications. The study of fatigue resistance is of special interest, since this phenomenon is present in many application fields.

1.2 Justification

The fatigue characterization of the composite materials under the ASTM D7791 standard, allows knowing a design requirement of vital importance for the manufacture of functional parts such as fatigue resistance.

Obtaining S-N curves, for different configurations of composite materials (obtained by varying printing parameters such as fibre reinforcing material and its quantity, fibre deposition angle and matrix filling pattern), will allow to know which configuration is optimal in each application according to the design requirements of the product to be manufactured.

In addition, this study encourages the development of research projects at the School of Mechanical Engineering, since these reinforced composites are widely used in applications such as biomechanics, auto parts manufacturing and aerospace engineering, which are current research lines of the GIEMA group, linked to the university.

2 Objectives

2.1 General objetive

Characterize the uni-axial fatigue properties under tensile load as stipulated in the ASTM D7791 standard which contemplates 3D printed elements using FMD technology (fused deposition modelling), which have a nylon matrix and reinforcements in fiberglass, kevlar or carbon fibres.

2.2 Specific objetives

- Experimentally determine the stress curve versus load cycles (S-N) on specimens printed with a nylon matrix, using triangular and hexagonal filling patterns, each with a fill pattern density of 20% and 50%.
- Experimentally determine the stress curve versus load cycles (S-N) in specimens printed with a nylon matrix reinforced with isotropic layers made of glass fibres, kevlar and continuous carbon fibres with orientation patterns of 0, 45 and 90 degrees.
- Experimentally determine the stress curve versus load cycles (S-N) in specimens printed with a nylon matrix reinforced by concentric rings made of continuous fibres of the determined optimum material.
- Realize a Weibull distribution study on the (S-N) graphs obtained, which allows analysing and comparing the results in the tests by varying the different printing patterns mentioned.

3 Materials and methods

Uniaxial tensile tests performed in previous studies were carried out according to ASTM D638 standard. Type IV specimen dimensions in ASTM D638-14 standard were used. The specimens were printed in the Mark Two printer of the Mark Forged Company. The tests were performed at a strain velocity of 5 mm/min, grips distance of 28 millimetres and the longitudinal strain and transversal section contraction were determinate using the LVDT and the laser extensometer LX500, respectively. The test machine used for the tensile tests was the MTS Bionix Tabletop model 370.

Table 1. Testing parameters for uniaxial tensile tests

Testing parameters	
Testing strain speed	5 (mm/min)
Distance between grips	28 (mm)
Sampling frequency	5 (Hz)

The printing parameters used in the Mark Two printer for manufacturing both tensile and fatigue tests specimens are the same and are explained in detail below.

The characterization of fatigue properties under uniaxial tension load is performed under the ASTM D7791 standard - Uniaxial Fatigue Plastic Properties - procedure A, for rigid and semi-rigid plastics, with a stress ratio value (R) equal to 0.1, in tensile-tensile condition.

Materials tensile strength values were determined in a tensile stress test according to ASTM D638 standard. These values were taken from previous studies performed to same specimens with the same printer patron configuration as specimens studied in fatigue tests.

The aim of these tests is to estimate the life/stress curve vs. the number of cycles (S vs N), under the condition of temporary life of composite materials.

Specimens to be tested have a nylon matrix with triangular and hexagonal filling patterns; fill densities of 50% or 20% are used.

The types of reinforcement used in the nylon matrix are:

• Isotropic layers of fibreglass, carbon fibre and Kevlar as reinforcement material at orientations of 0, 45, and 60 degrees.

• Concentric rings of continuous fibres of fibreglass, carbon fibre and Kevlar.

Four (4) levels of percentages of the ultimate tensile stress will be used for the tests (95%, 90%, 85% and 80%). For the construction of the S-N curve, 5 specimens are tested in each one of load levels.

The geometry of the specimens is standardized according to ASTM D638-14 standard, selecting the type I of specimens for rigid plastic materials, semi-rigid or reinforced composites, where the thickness of the material to be tested does not exceed 7 mm (0.28 in.). The MarkforgedOne 3D printer is used for the printing of the specimens.

The test machine used for the dynamic test is the MTS Bionix Tabletop model 370, with a load cell of 25 KN capacity and an approximate displacement of 57 mm, see Figure 1. The selected frequency is 5 Hz in agreement with ASTM D7791.

Figure 1. MTS Bionix Tabletop machine.

The specimen geometry was exported as a stereolithographic file (STL) to the software EIGER, which control the Mark Forged printer. The software allows changing several printing patterns such as fill percentage, filling pattern and number of nylon or fibre reinforcement layers, as shown in Table 2.

Fracture interface of the specimens was observed using an SEM, a JEOL, JSM 6490-LV Scanning Electron Microscope was used with different magnifications.

Table 2. Printing patterns for nylon matrixes.

Layer height (mm)	0,1
Filling percentage (%)	20 , 50
Filling pattern	Triangular, Hexagonal
Filling layers number	24
Walls number	2
Upon layers number	4
Below layers number	4
Total layers	32

Table 3. Printing patterns for isotropous layers specimens.

Layer height (mm)	0,1
Filling percentage (%)	20
Filling pattern	Triangular
Fibre layers number	6
Filling fibre kind	Isotropous
Fibre angle	0°, 45°, 90°
Filling layers number	18
Walls number	2
Upon layers number	4
Below layers number	4
Total layers	32

Table 4. Printing patterns for concentric rings.

Layer height (mm)	0,1
Filling porcentage (%)	20
Filling pattern	Triangular
Fibre layers number	4, 2
Filling fibre kind	Concentric rings
Concentric rings	2, 4
Filling layers number	24
Walls number	2
Upon layers number	4
Below layers number	4
Total layers	32

4 Results and discussion

The results presented in this section are the following:

4.1 Uniaxial tensile test

The uniaxial tensile tests performed in previous studies show the ultimate tensile stress (Sut) and the strain of the specimens. The aim was to determinate in each stage of the investigation which was the optimal printing pattern based on the (Sut).

Figure 2 shows the comparison between the nylon matrices printed at 20% of the filling density at different filling patterns. The results determinate that triangular filling pattern had the higher ultimate tensile stress value.

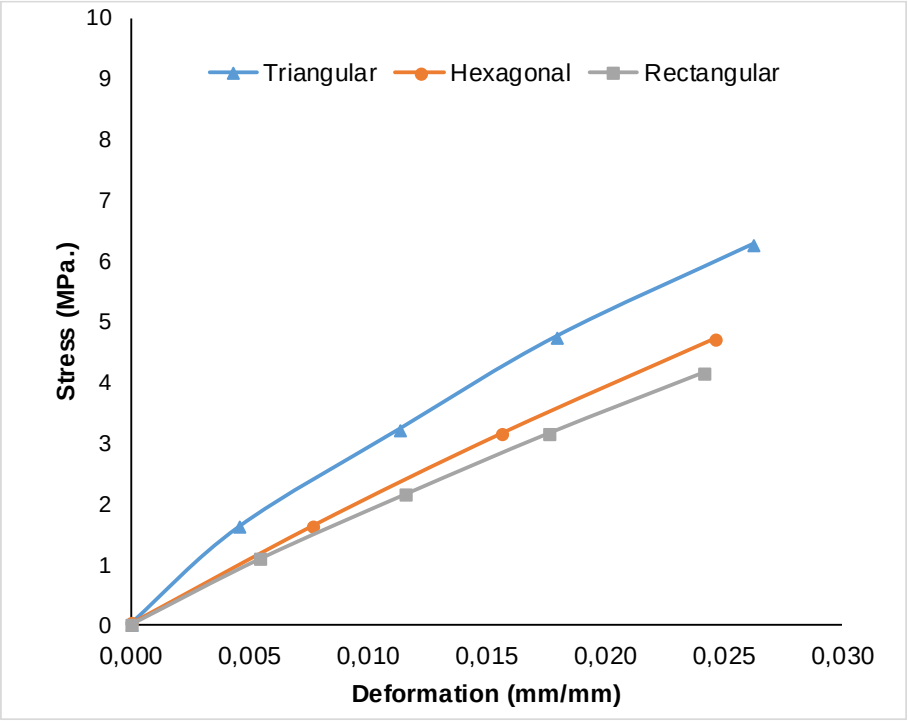

Figure 2. Uniaxial tensile test curves, pattern and fill percentage selections.

The Figure 3 shows the comparison between the specimens with isotropic layers filled in different fibre angle orientation, all of them were printed in fibreglass. The results showed that the optimal fibre angle orientation in the isotropic layers was at 0 degrees.

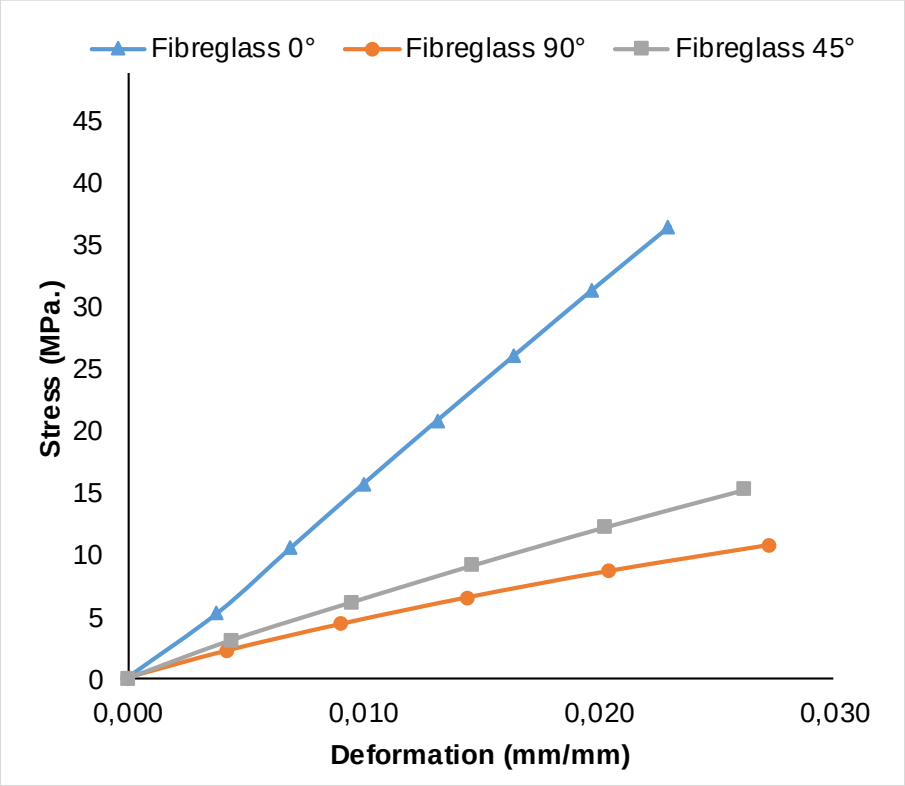

Figure 3. Uniaxial tensile test curves, nylon matrix with the triangular filling pattern, 20% of filling percentage, fibreglass as reinforcement material at 0°, 45° and 60° orientation.

Figure 4 shows the comparison between the different materials used in the isotropic layers at the 0 degrees fibre orientation. Kevlar, Carbon and Glass fibres were tested. The results showed that carbon fibre isotropic layers had the higher ultimate tensile stress value.

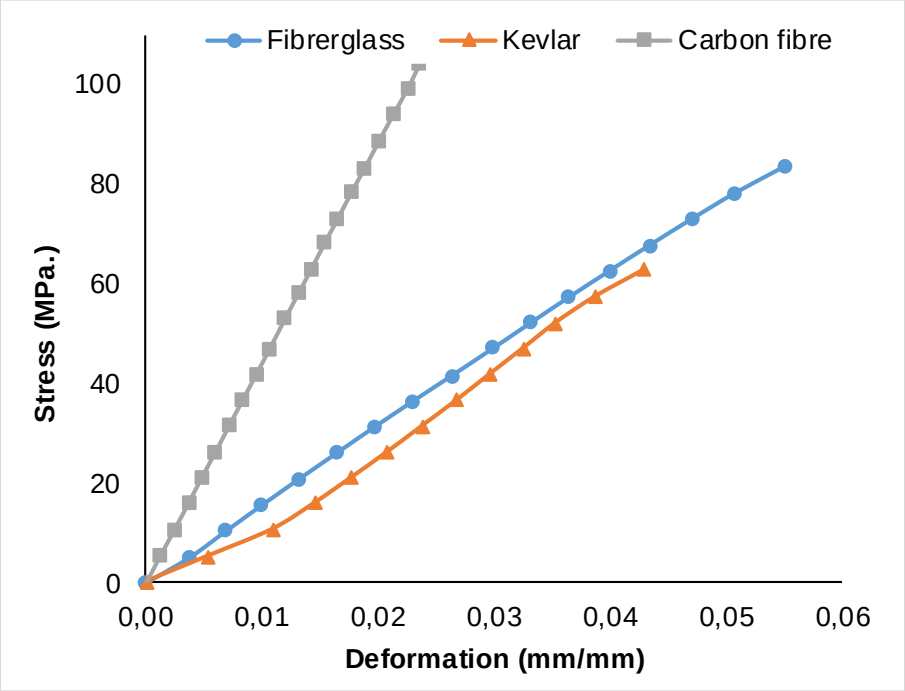

Figure 4. Uniaxial tensile test curves, nylon matrix with the triangular filling pattern, 20% of filling percentage, Kevlar, carbon and glass fibres as reinforcement material at 0° orientation.

The Figure 5 shows the comparison between two different reinforcement configurations. Concentric rings reinforcement printed in Carbon fibre were manufactured in two different configurations, two rings and four layers or four rings and two layers. The results showed that the four layers and two rings configuration presented the higher ultimate tensile stress value.

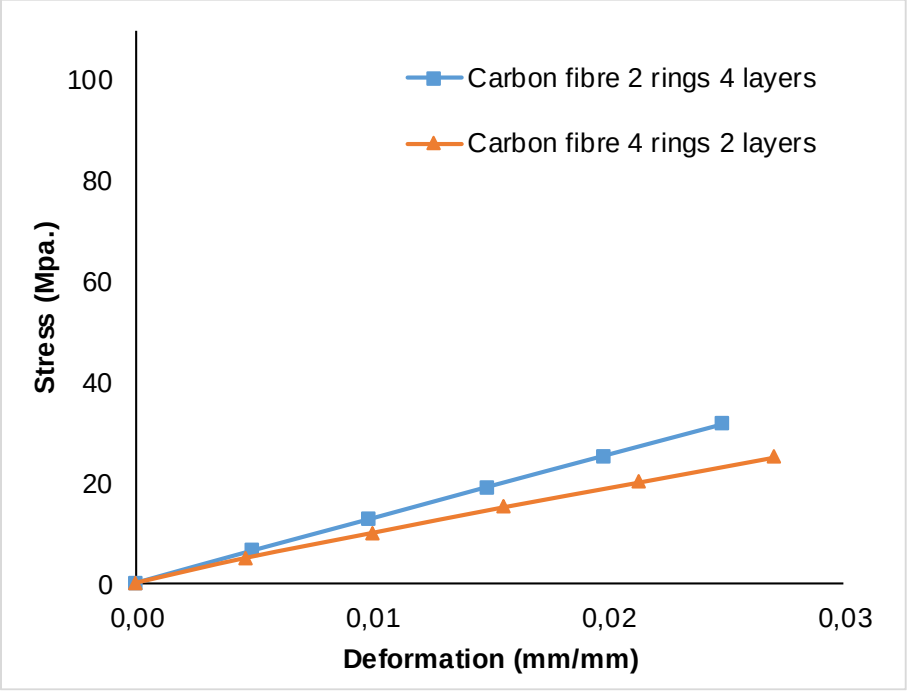

Figure 5. Uniaxial tensile test curves, nylon matrix with the triangular filling pattern, 20% of filling percentage, carbon fibre 2 rings 4 layers reinforcement and carbon fibre 4 rings 2 layers reinforcement.

4.2 Effects of the filling percentage and the fill pattern of the matrix

In the first stage of the experiment, the filling percentage and pattern of the nylon matrix are varied, as shown in Table 5.

Table 5. Variables of the experiment in the first stage.

Matrix fill (%)	Pattern fill	Load levels (%)
20, 50	Triangular, Hexagonal	80, 85, 90, 95

For the representation of the material stress in the S-N curve, there are different models that adjust the data in such a way that a certain level of reliability can be obtained.

In this paper, we present the Basquin´s Model, which relate logarithmically the stress on the material with the number of cycles.

The Basquin´s equation is the following:

$\log(S) = \beta \log(N) + \alpha$	(1)

To obtain a better precision in the estimation of the S-N curves, under the recommendation of the D3479 standard, the Weibull distribution is selected as the statistical method for the adjustment of the data obtained on each load level test.

By adjusting the data to this statistical tool, we can obtain a precise mean for the cycles of the material in its respective load level.

The goodness test for the data fit analysis in each of the Weibull analyzes was done under the Kolmogorov-Smirnov test, with confidence intervals of 90 to 95 percent, thus with a P-Value higher than 0.05 - 0,1 we cannot reject the hypothesis that the data adjust to a Weibull distribution, i.e., the data fit the Weibull model with a 90-95 percent reliability.

Using the STATGRAPHICS® software, the Weibull analysis is performed, and curves are constructed for each respective fill percentage and fill pattern of the matrix, under the above-stipulated loads.

The data obtained from the experiments related to the specimens for each of the patterns and filling percentage are the following:

Table 6. Data obtained from the experiments related to the specimens with hexagonal filling pattern and 50% of filling percentage and Weibull analysis performed using STATGRAPHICS®.

Hexagonal 50%							
Samples	Stress S, (MPa.)	Stress percentage	Cycles (N)	Weibull analysis			
				P-Value	Mean cycles	Alpha	Beta
1	12,83173	80%	459	1	386,106	8,39	409,1
2			295				
3			393				
4			360				
5			420				
1	13,63365	85%	267	1	262,027	40,1	265,7
2			267				
3			271				
4			245				
5			258				
1	14,4357	90%	269	1	249,1	21,4	255,4
2			250				
3			245				
4			230				
5			253				
1	15,2375	95%	165	1	160,358	7,3	171,1
2			136				
3			196				
4			128				
5			176				

Table 7. Data obtained from the experiments related to the specimens with triangular filling pattern and 20% of filling percentage and Weibull analysis performed using STATGRAPHICS®.

Triangular 20%							
Samples	Stress S, (MPa.)	Stress percentage	Cycles (N)	Weibull analysis			
				P-Value	Mean cycles	Alpha	Beta
1	12,46394	80%	597	1	551,327	2,97	617,6
2			725				
3			315,5				
4			427,5				
5			528				
1	13,23317	85%	397,5	0,0548	354,281	3,04	396,5
2			205				
3			463,5				
4			185				
5			363,5				
1	14,01923	90%	370	1	340,075	18,75	349,9
2			344				
3			351				
4			325				
5			311,5				
1	14,80529	95%	221,5	1	232,206	17,8	239,3
2			248,5				
3			250				
4			210,5				
5			230				

Table 8. Data obtained from the experiments related to the specimens with triangular filling pattern and 50% of filling percentage and Weibull analysis performed using STATGRAPHICS®.

Triangular 50%							
Samples	Stress S, (MPa.)	Stress percentage	Cycles (N)	Weibull analysis			
				P-Value	Mean cycles	Alpha	Beta
1	13,67115	80%	538	0,066	401,915	5,34	436,1
2			359				
3			343				
4			440				
5			335				
1	14,52548	85%	363	1	384,838	15,6	398
2			382				
3			426				
4			353,5				
5			402,5				
1	15,38005	90%	328	1	274,883	8,7	290,8
2			229,5				
3			267,5				
4			298				
5			253				
1	16,1863	95%	219	1	211,178	15,8	218,3
2			223				
3			196				
4			185,5				
5			230				

As an example of the procedure for the construction of the curves, the triangular pattern with 20 percent fill is shown in Figure 6.

The S-N curve obtained by adjusting the above data to the Basquin´s Model is the following:

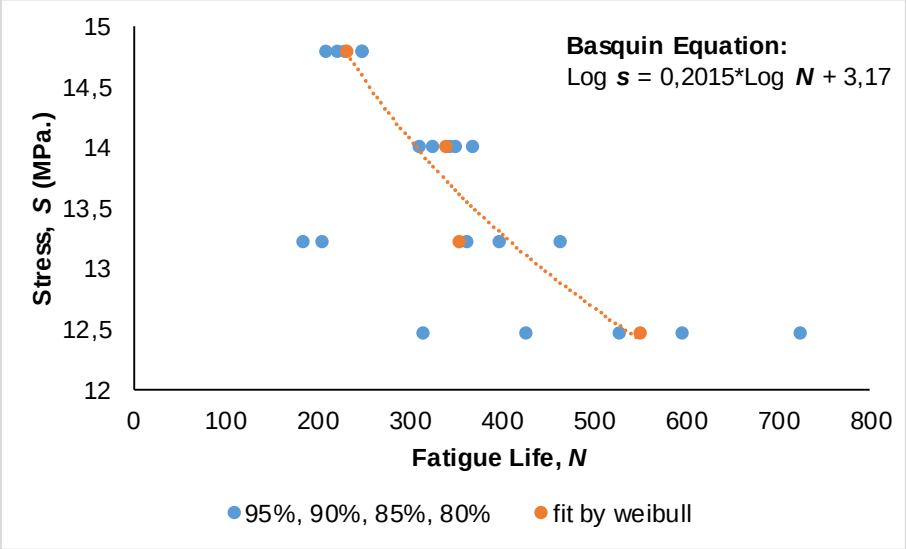

Figure 6. S – N curve fitted to the Basquin´s model, for nylon matrix with triangular filling pattern and 20% of filling percentage.

The correlation coefficient for the data obtained under the Weibull analysis and then adjusted to the Basquin's model is -0.9617, which indicates a strong relationship between the variables and in conclusion a good fit of the model to the obtained data.

Developing this same analysis for each of the variables mentioned in Table 5. The results obtained in the first stage are the following:

For the nylon matrices with the patterns and filling percentage, the following S-N curves are obtained according to the stipulated load levels:

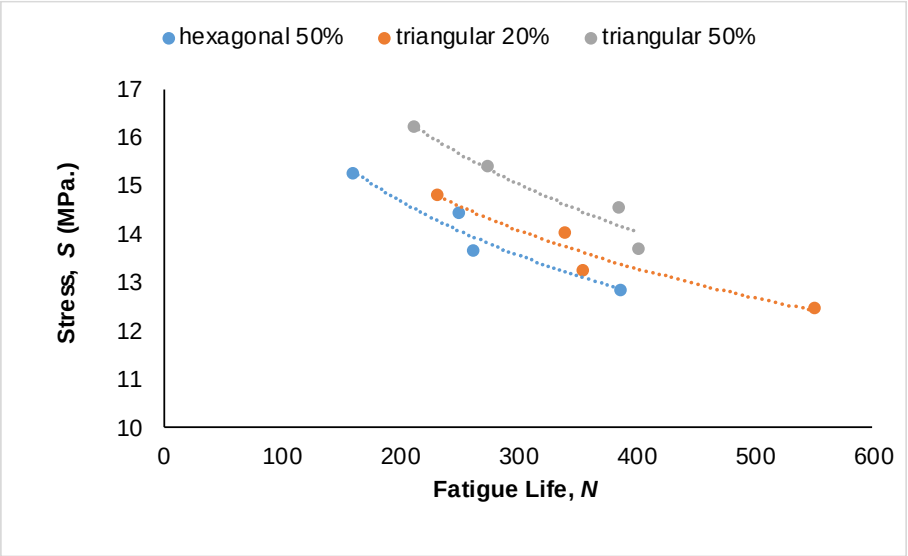

Figure 7. S-N curves, pattern and fill percentage selections.

The alpha and beta coefficients of the Basquin's model that represent each of the previous curves shown in Figure 7, for each of the percentages and fillings of the matrix are:

Table 9. alpha and beta coefficients of the Basquin's model for each of the nylon matrices with the patterns and filling percentage.

Material	Alpha	Beta
Hexagonal 50%	3,735	-0,198
Triangular 20%	3,792	-0,202
Triangular 50%	4,020	-0,230

It is observed from the Figure 7 than the nylon matrix with a percentage of filling of 20% and triangle filling pattern presents the optimum performance S-N curve, since comparatively, under the characteristic loads of the experiment, it presents a greater number of life cycles before the rupture of the material, which translates into a curve of semi-bell shape wider than the others.

The specimens printed without fibre reinforcement showed an elastic behaviour. Most of these specimens had a yield failure, their elastic strain overcome the test machine displacement. Only a few specimens filled at 50% with triangular patron showed a fracture failure.

4.3 Effects of the fibre orientation

The first objective in the second phase of the experiment is to determine through the use of fibreglass as reinforced material, the optimum orientation angle of the fibres, with which the nylon matrix increases its resistance to fatigue, once this variable is determined, different reinforcement materials are tested, and it is analyzed which of them presents the best performance in the S-N curve.

Table 10. Variables of the experiment in the second stage.

Matrix fill (%)	Pattern fill	Reinforced material	Fibres orientation (°)	Load levels (%)
20	Triangle	Fibreglass	0, 45, 60	80, 85, 90, 95

The second phase of the experiment is developed under the same methodology shown in section 3.1, for the obtaining of the percentage and optimal fill pattern.

The data obtained from the experiments related to the specimens for each of the fibre orientation are the following:

Table 11. Data obtained from the experiments and Weibull analysis performed using STATGRAPHICS®, related to the specimens with triangular filling pattern and 20% of filling percentage and fibreglass as reinforced material at 0° orientation.

Glassfibre 0°							
Samples	Stress ***S*** , (MPa.)	Stress percentage	Cycles (***N***)	Weibull analysis			
				P-Value	Mean cycles	Alpha	Beta
1	98,798	80%	510	1	517,519	27,8	527,8
2			503				
3			503				
4			550				
5			527				
1	105,048	85%	317	1	280,558	6,9	300,3
2			234				
3			259				
4			348				
5			246				
1	111,202	90%	176	1	150,1	5,7	162,3
2			170				
3			114				
4			182				
5			103,5				
1	117,380	95%	30,5	1	56,61	2,2	64
2			42				
3			88				
4			27,5				
5			93				

Table 12. Data obtained from the experiments and Weibull analysis performed using STATGRAPHICS®, related to the specimens with triangular filling pattern and 20% of filling percentage and fibreglass as reinforced material at 45° orientation.

Glassfibre 45°							
Samples	Stress ***S*** , (MPa.)	Stress percentage	Cycles (***N***)	Weibull analysis			
				P-Value	Mean cycles	Alpha	Beta
1	20,692	80%	310,5	1	299,026	4,5	327,7
2			180,5				
3			415,5				
4			280				
5			307,5				
1	21,986	85%	223	1	252,314	8,6	266,9
2			270				
3			302				
4			214				
5			254				
1	23,279	90%	123	1	149,7	6,22	161,1
2			184				
3			105				
4			166				
5			167				
1	24,567	95%	127	1	82,371	3	92,2
2			46				
3			52				
4			84				
5			101				

Table 13. Data obtained from the experiments and Weibull analysis performed using STATGRAPHICS®, related to the specimens with triangular filling pattern and 20% of filling percentage and fibreglass as reinforced material at 60° orientation.

Glassfibre 60°							
Samples	Stress ***S*** , (MPa.)	Stress percentage	Cycles (***N***)	Weibull analysis			
				P-Value	Mean cycles	Alpha	Beta
1	19,615	80%	537,5	0,0625	503,964	13,1	524,3
2			494				
3			561,5				
4			412				
5			508				
1	20,841	85%	419	1	440,487	22,8	451,1
2			436,5				
3			471				
4			418,5				
5			459				
1	22,067	90%	342	1	310,519	9,3	327,5
2			361				
3			259				
4			317,5				
5			270,5				
1	23,293	95%	83	1	94,247	5,6	101,9
2			125				
3			100,5				
4			85				
5			79,5				

With the variables established in Table 10, Table 11, Table 12, Table 13. The S-N curves obtained from the Basquin's model for each of the fibres orientation are the followings:

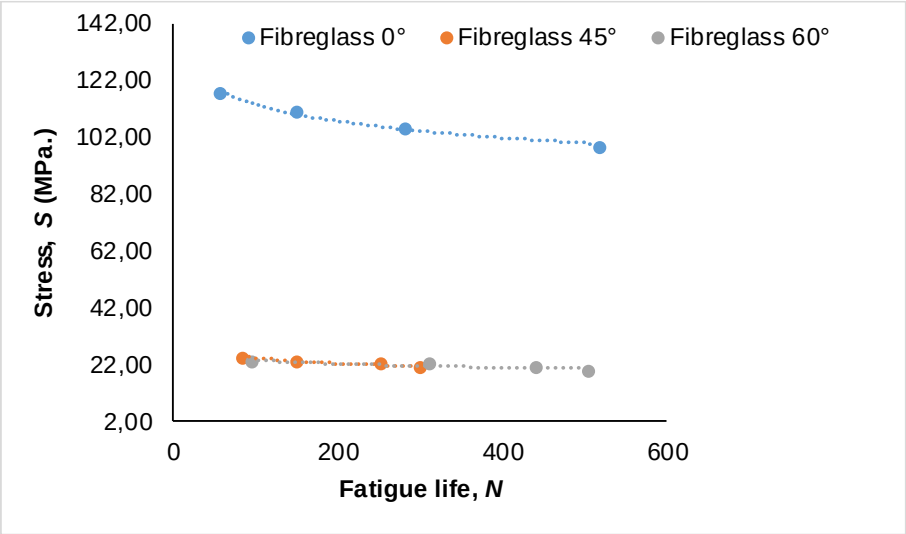

Figure 8. S – N curves fitted to the Basquin's model for nylon matrix with the triangular filling pattern, 20% of filling percentage, fibreglass as reinforcement material at 0°, 45° and 60° orientation.

The alpha and beta coefficients of the Basquin's model that represent each of the previous curves shown in Figure 8, for each of the fibres orientation are the followings:

Table 14. alpha and beta coefficients of the Basquin's model for each of the nylon matrices with the patterns and filling percentage.

Material	Alpha	Beta
Glassfibre 0°	5,087	-0,078
Glassfibre 45°	3,754	-0,123
Glassfibre 60°	3,557	-0,087

From the previous S-N curves shown in Figure 8, constructed with the characteristic loads, it is observed that with the orientation of **0** degrees of the fibres, specimens show a better performance, increasing the number of cycles before rupture of the specimen.

As an observation for this phase of the experiment, as the angle varied from zero degrees, the material begins to fail due to yield and not rupture, in addition to this the nylon matrix lengthened in a similar way as it did in the tests without any reinforcing fibre.

The break failures observed in the specimens reinforced with glass fibre orientated at 60 degrees (and some specimens with glass fibre orientated at 45 degrees) reinforcement at load percentages of 85% and 80% of the ultimate tensile stress resistance, were similar to the failures in the specimens without fibre reinforcement. It can be observed that the greater the inclination of the fibre, more percentage of the load is absorbed by the nylon matrix and it cause the nylon matrix deformation.

4.4 Effects of the fibre reinforcement material

Once the orientation of the fibres has been determined, other materials are used to reinforce the nylon matrix and its behaviour in the S-N curve is observed.

Table 15 shows the reinforcement materials with which the different tests will be made for each of the stipulated loads

Table 15. Variables of the experiment, reinforcement material determination.

Matrix fill (%)	Pattern fill	Reinforced material	Fibres orientation (°)	Load levels (%)
20	Triangle	Carbon fibre, Kevlar	0	80, 85, 90, 95

The data obtained from the experiments related to the specimens for each of the reinforced fibre material are the following.

Table 16. Data obtained from the experiments and Weibull analysis performed using STATGRAPHICS®, related to the specimens with triangular filling pattern and 20% of filling percentage and carbon fibre as reinforced material at 0° orientation.

Carbon fibre 0°							
Samples	Stress ***S*** , (MPa.)	Stress percentage	Cycles (***N***)	Weibull analysis			
				P-Value	Mean cycles	Alpha	Beta
1	132,212	80%	72023	1	80074,6	6,8	85729,2
2			75934				
3			93629				
4			97116,5				
5			60995,5				
1	140,385	85%	41189	1	287570	2,3	32456,1
2			4936				
3			28635				
4			32612				
5			38520				
1	148,558	90%	10392,5	0,08	9351,51	3,3	10420,3
2			14579				
3			8145				
4			5987				
5			7605				
1	156,971	95%	1395	0,39	968,479	1,7	1082,9
2			202				
3			350,5				
4			1452				
5			1463				

Table 17. Data obtained from the experiments and Weibull analysis performed using STATGRAPHICS®, related to the specimens with triangular filling pattern and 20% of filling percentage and kevlar fibre as reinforced material at 0° orientation.

Kevlar 0°							
Samples	Stress ***S*** , (MPa.)	Stress percentage	Cycles (***N***)	Weibull analysis			
				P-Value	Mean cycles	Alpha	Beta
1	88,846	80%	876	1	1428,1	2,5	1609,5
2			2532				
3			1600				
4			1074,5				
5			1024				
1	94,471	85%	112	1	242,327	2,1	273,6
2			433				
3			322				
4			223,5				
5			114				
1	99,952	90%	48	1	78,23	2,2	88,3
2			69,5				
3			67,5				
4			152				
5			51,5				
1	105,529	95%	10	1	16,074	1,5	17,8
2			14				
3			2				
4			26				
5			29				

With the variables established in Table 15, Table 16, Table 17, the S-N curves obtained from the Basquin's model for each of the reinforced fibre material are the followings.

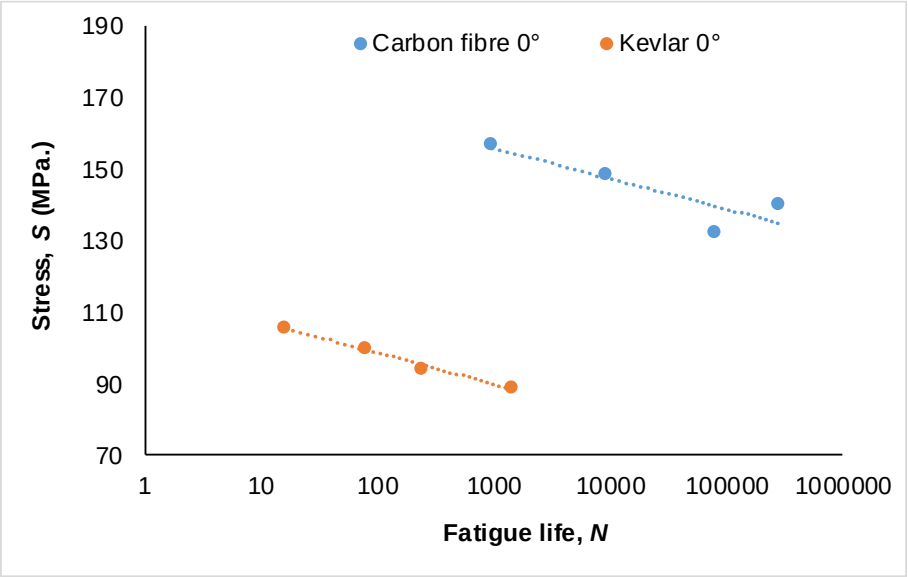

Figure 9. S – N curves fitted to the Basquin's model for nylon matrix with the triangular filling pattern, 20% of filling percentage, carbon fibre and Kevlar fibre as reinforcement material at 0° orientation.

The alpha and beta coefficients of the Basquin's model that represent each of the previous curves shown in Figure 9, for each of the reinforced fibre material are the followings:

Table 18. alpha and beta coefficients of the Basquin's model for each of the nylon matrices with the patterns and filling percentage.

Material	Alpha	Beta
Carbon fibre 0°	5,222	-0,025
Kevlar 0°	4,769	-0,039

Finally, it is concluded, based on the S-N curves shown in Figure 9, for a specimen with: nylon matrix, percentage of filling of **20**%, triangle pattern filling, the best performance is achieved when the material is reinforced with carbon fibre fibres at an orientation of **zero** degrees, thus increasing the number of cycles for each of the characteristic loads of the experiment.

A considerable number of specimens reinforced with carbon fibre (isotropic layers at 0 degrees and concentric rings) break in the change of the transversal area section. It was observed that in most of the specimens, the fibre reinforcement in this zone was absent, especially in the specimens reinforced with concentric rings.

The specimens with carbon fibre reinforcement that show greater cycle's number had fibre reinforcement in the change of the transversal area section.

4.5 Effects of the material and number of concentric rings

The aims in the last phase of the experiment consist in determining what is the optimum number and of ring-type reinforcements for the same nylon matrix with the previously established characteristics.

The optimum number of ring-type reinforcements is determined by means of the construction of the S-N curve, for the next mentioned characteristic as shown in Table 19.

Table 19. Variables of the experiment in the third stage.

Matrix fill (%)	Pattern fill	Reinforced material	Number of ring-type reinforcements	Load levels (%)
20	Triangle	carbon fibre	2, 4	80, 85, 90, 95

The data obtained from the experiments related to the specimens for each of the number of ring-type reinforcements are the following

Table 20. Data obtained from the experiments and Weibull analysis performed using STATGRAPHICS®, related to the specimens with triangular filling pattern and 20% of filling percentage and carbon fibre 2 rings 4 layers reinforced material.

Carbon fibre 2 rings 4 layers							
Samples	Stress ***S*** , (MPa.)	Stress percentage	Cycles (***N***)	Weibull analysis			
				P-Value	Mean cycles	Alpha	Beta
1	90,865	80%	40674,5	0,0823	40232,8	8,43	42613,5
2			32897				
3			47635				
4			35166,5				
5			44551,5				
1	96,442	85%	2052	1	27222,6	0,74	22582,6
2			81799				
3			5614				
4			43925				
5			3439				
1	102,163	90%	38075,5	0,0581	57770,3	0,5	28578,9
2			3,5				
3			72050				
4			15789				
5			65245				
1	107,692	95%	425	0,0614	365,356	3,2	408,1
2			566				
3			293,5				
4			191				
5			346,5				

Table 21. Data obtained from the experiments and Weibull analysis performed using STATGRAPHICS®, related to the specimens with triangular filling pattern and 20% of filling percentage and carbon fibre 4 rings 2 layers reinforced material.

Carbon fibre 4 rings 2 layers							
Samples	Stress ***S*** , (MPa.)	Stress percentage	Cycles (***N***)	Weibull analysis			
				P-Value	Mean cycles	Alpha	Beta
1	51,923	80%	35321	0,2617	27510,4	1,95	31026
2			31857				
3			2735				
4			33277,5				
5			38240				
1	55,048	85%	9070,5	0,9167	4250,93	0,69	3328,9
2			7675				
3			86				
4			3173,5				
5			246				
1	58,413	90%	5019	0,9339	940,721	0,34	170,531
2			16				
3			95				
4			1				
5			11				
1	61,538	95%	211	0,72	100,614	1,13	105,179
2			102				
3			115				
4			3				
5			78				

With the variables established in Table 20 and Table 21, the S-N curves obtained from the Basquin's model for each of the reinforced ring-type materials are the followings:

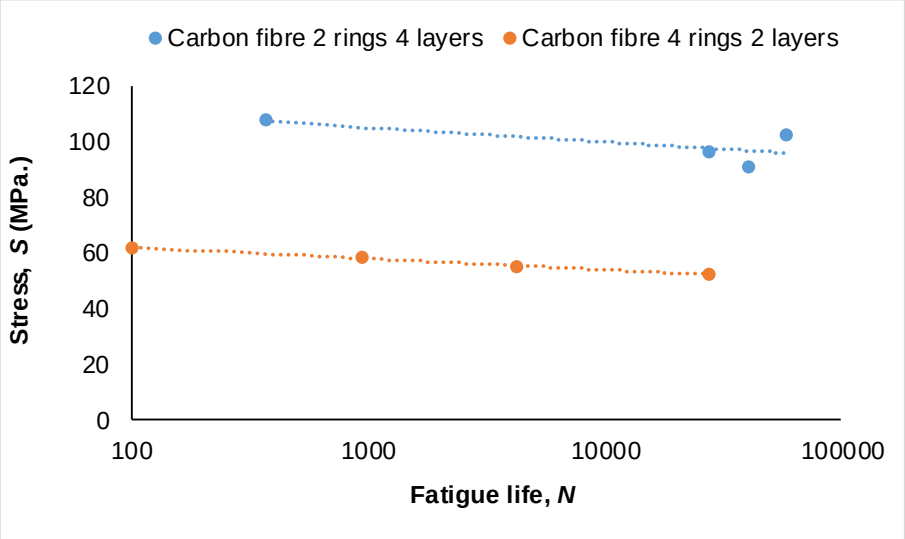

Figure 10. S-N curve, selection of number of ring-type reinforcement.

The alpha and beta coefficients of the Basquin's model that represent each of the previous curves shown in Figure 10, for each of the numbers of ring-type reinforcements are the followings:

Table 22. alpha and beta coefficients of the Basquin's model for each of the nylon matrices with the patterns and filling percentage.

Material	Alpha	Beta
Carbon fibre 2 rings 4 layers	4,80342	-0,022015
Carbon fibre 4 rings 2 layers	4,268	-0,031

Based on Figure 10, it is concluded that the best behaviour of the specimen is achieved when it is reinforced with **2 rings 4 layers** ring-type reinforcement material, thus increasing the number of cycles for each of the characteristic loads of the experiment.

4.6 Fracture interface observation after fatigue testing

The thickness of the nylon matrix in the central part and the reinforcing layers in the upper part fused between the thickness of the nylon matrix are shown for the Kevlar fibre reinforcing material at Figure 13 and for the carbon fibre reinforcing material at Figure 11 and Figure 12.

it is observed in Figure 11 and Figure 13, the fracture in the upper part of the nylon matrix, where some incipient beach lines are formed that can be attributed to the dynamism in the fatigue tests. Comparatively, it is observed that the beach lines are present in the nylon matrix but not in the reinforcing fibres, since this is a more ductile material.

With respect to the reinforcement fibres present in the specimens, it can be observed that the fracture of the fibres was more uniform in the specimen tests at 80% of the ultimate load of rupture (Sut), as shown in Figure 11, for the nylon matrix specimen with carbon fibre as reinforcement material.

In the specimens tested at 95% of the (Sut), it is observed how some fibres were longer than others, due to the overload. As show in Figure 12 for nylon matrix specimen reinforced with carbon fibre.

Comparatively, it can be observed that in the specimens reinforced with Kevlar fibre, the fibres are more continuous, as threads, since Kevlar is a more ductile material than carbon fibre.

In the fracture of the specimens reinforced with Kevlar fibre, the formation of knots in the fibres can be seen Figure 14, while in the specimens reinforced with carbon fibre, the fibres break and their orientation at 0 ° is conserved almost completely, as shown in Figure 11.

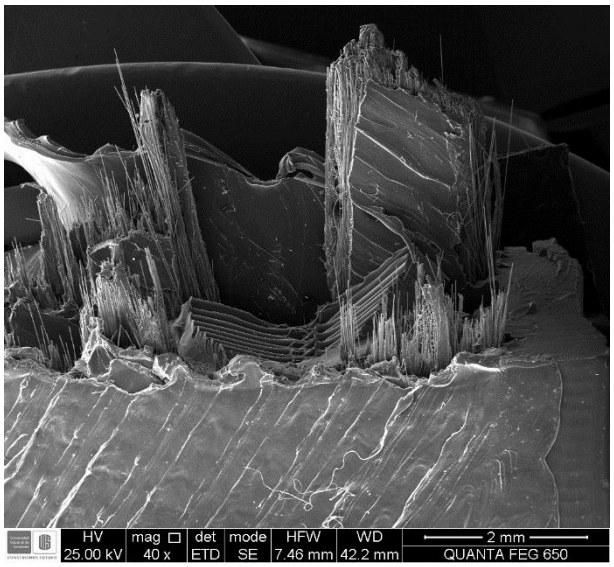

Figure 11. SEM image shows the fracture of the specimen with the triangular filling pattern, 20% of filling percentage and carbon fibre as reinforced material at 0° orientation at 80% of (Sut).

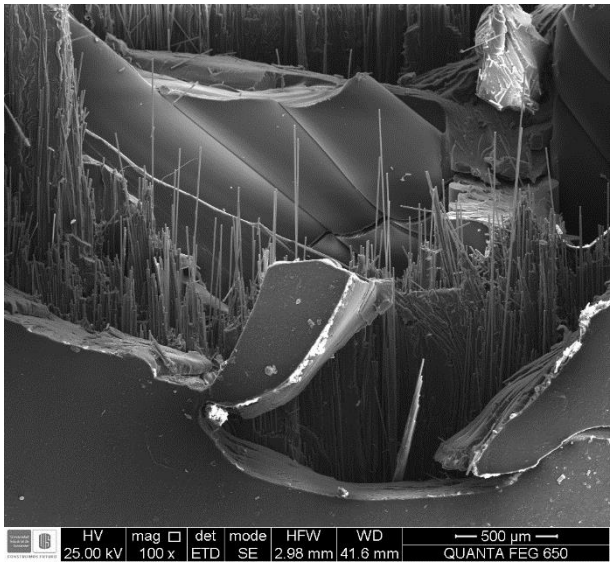

Figure 12. SEM image shows the fracture of the specimen with the triangular filling pattern, 20% of filling percentage and carbon fibre as reinforced material at 0° orientation at 95% of (Sut).

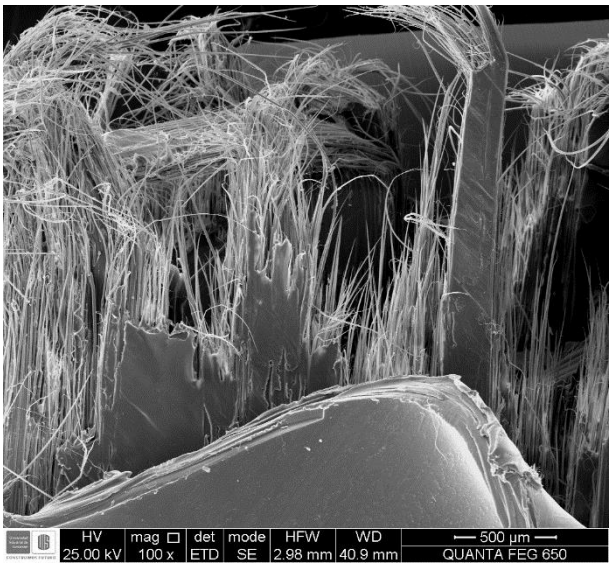

Figure 13. SEM image shows the fracture of the specimen with the triangular filling pattern, 20% of filling percentage and Kevlar fibre as reinforced material at 0° orientation at 80% of (Sut).

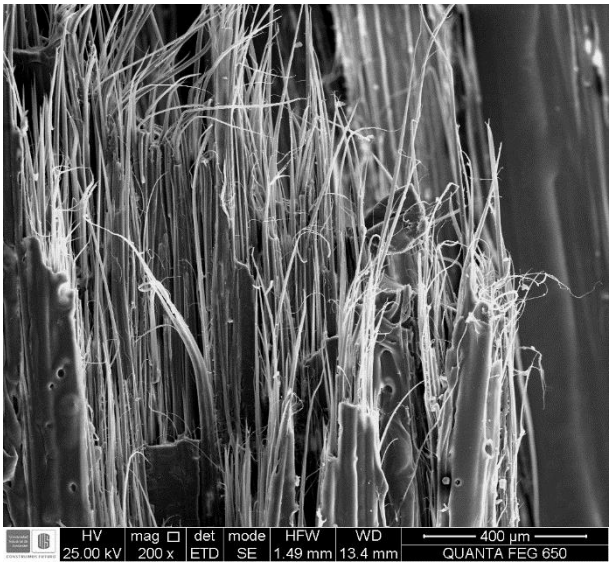

Figure 14. SEM image shows the fracture of the specimen with the triangular filling pattern, 20% of filling percentage and Kevlar fibre as reinforced material at 0° orientation at 95% of (Sut).

5 Conclusions

It was observed that the optimal pattern of filling for the nylon matrix without reinforcement was triangular and 20% of filling percentage. Comparatively this configuration tolerates approximately 100 more load cycles N in the 95% of the Sut and 200 more load cycles N in the 80% of the SuT. The specimens printed without fibre reinforcement showed an elastic behavior. Most of these specimens had a yield failure, and their elastic strain overcome the test machine displacement.

The results showed that the optimal fibre angle orientation was at 0 degrees. Due to the stiffness of this configuration, comparatively with the 45 degrees and 60 degrees configurations, approximately 100 MPa or more was tolerated in each one of the Sut percentages. The number of the load cycles N was almost the same for all the configurations.

The break failures observed in the specimens reinforced with glass fibre orientated at 60 degrees (and some specimens with glass fibre orientated at 45 degrees) reinforcement at load percentages of 85% and 80% of the ultimate tensile stress resistance, were similar to the failures in the specimens without fibre reinforcement.

The results concluded that the nylon matrix reinforced with carbon fibre layers oriented at 0° degrees presents the better fatigue response. The number of load cycles N was superior in each of the Sut percentages as shown in Figure 9. A considerable number of specimens reinforced with carbon fibre (isotropic layers at 0 degrees and concentric rings) break in the change of the transversal area section. The specimens with carbon fibre reinforcement that show greater cycle's number had fibre reinforcement in the change of the transversal area section.

The concentric rings reinforcement configuration of 2 rings, 4 layers, showed a better fatigue response that the 4 rings 2 layers configuration. Approximately 40 MPa or more was tolerated in each one of the Sut percentages. For the 90 % and 95% of Sut the 2 rings 4 layers configuration present more load cycles $\boldsymbol{N}$, as shown in Table 20 and Table 21.

The effect of the humidity in the specimens was observed. A specimen per each load percentage in all the experiments was left at atmospheric humidity conditions. The results showed that the specimens without fibre reinforcement were more susceptible to the effect of the humidity than the specimens with fibre reinforcement. These specimens showed yield failures at lower load cycles than the specimens conserved at the humidity-controlled condition.

The results obtained from the experimentation presented satisfactory results and make viable the continuation of the experimentation in this field. Seeking to acquire new knowledge in the continuous fibre reinforced thermoplastic composites, new studies about different parameters such as combined loads and new patterns and percentage of filling are needed.

References

Ahn, S., Montero, M., Odell, D., Roundy, S., & Wright, P. K. (2002). Anisotropic material properties of fused deposition modeling ABS. *Rapid Prototyping Journal*, *8*(4), 248–257. https://doi.org/10.1108/13552540210441166

Alimardani, M., Toyserkani, E., & Huissoon, J. P. (2007). Three-dimensional numerical approach for geometrical prediction of multilayer laser solid freeform fabrication process. *Journal of Laser Applications*, *19*(1), 14–25. https://doi.org/10.2351/1.2402518

Basquin, O. H. (n.d.). The exponential law of endurance tests. *Proceedings of the American Society for Testing and Materials*, *10*(2), 625–630.

Bhuiyan, F. H., & Fertig, R. S. (2017). A Physics-Based Combined Creep and Fatigue Methodology, (January), 1–8. https://doi.org/10.2514/6.2017-0201

Brunbauer, J., & Pinter, G. (2015). Stiffness and strength based models for the fatigue-life prediction of continously fiber reinforced composites. *Material Science Forum*, *825*, 960–967. https://doi.org/10.4028/www.scientific.net/MSF.825-826.960

Der Klift, F. Van, Koga, Y., Todoroki, A., Ueda, M., Hirano, Y., & Matsuzaki, R. (2016). 3D Printing of Continuous Carbon Fibre Reinforced Thermo-Plastic (CFRTP) Tensile Test Specimens. *Open Journal of Composite Materials*, *6*(1), 18–27. https://doi.org/10.4236/ojcm.2016.61003

Dudek, P. (2013). FDM 3D printing technology in manufacturing composite elements. *Archives of Metallurgy and Materials*, *58*(4), 1415–1418. https://doi.org/10.2478/amm-2013-0186

Goel, A., Chawla, K. K., Vaidya, U. K., Chawla, N., & Koopman, M. (2009). Characterization of fatigue behavior of long fiber reinforced thermoplastic (LFT) composites. *Materials Characterization*, *60*(6), 537–544. https://doi.org/10.1016/j.matchar.2008.12.020

Hague, R., Campbell, I., & Dickens, P. (2003). Implications on design of rapid manufacturing. *Journal of Mechanical Engineering Science*, *217*(1), 25–30. https://doi.org/10.1243/095440603762554587

Kuhn, K., & Fertig III, R. S. (2016). A Physics-Based Fatigue Life Prediction for Composite Delamination Subject to Mode I Loading. *American Society for Composites Thirty-First Technical Conference*.

Leigh, S. J., Bradley, R. J., Purssell, C. P., Billson, D. R., & Hutchins, D. A. (2012). A Simple, Low-Cost Conductive Composite Material for 3D Printing of Electronic Sensors. *PLoS ONE*, *7*(11), 1–6. https://doi.org/10.1371/journal.pone.0049365

Li, N., Li, Y., & Liu, S. (2016). Rapid prototyping of continuous carbon fiber reinforced polylactic acid composites by 3D printing. *Journal of Materials Processing Technology*, *238*, 218–225. https://doi.org/10.1016/j.jmatprotec.2016.07.025

Mori, K., Maeno, T., & Nakagawa, Y. (2014). Dieless Forming of Carbon Fibre Reinforced Plastic Parts Using 3D Printer. *Procedia Engineering*, *81*(October), 1595–1600. https://doi.org/10.1016/j.proeng.2014.10.196

Ning, F., Cong, W., Qiu, J., Wei, J., & Wang, S. (2015). Additive manufacturing of carbon fiber reinforced thermoplastic composites using fused deposition modeling. *Composites Part B: Engineering*, *80*, 369–378. https://doi.org/10.1016/j.compositesb.2015.06.013

Standard terminology for additive manufacturing technologies. (2012). *ASTM F2792-12a*. West Conshohocken, PA.

Tekinalp, H. L., Kunc, V., Velez-Garcia, G. M., Duty, C. E., Love, L. J., Naskar, A. K., … Ozcan, S. (2014). Highly oriented carbon fiber-polymer composites via additive manufacturing. *Composites Science and Technology*, *105*, 144–150. https://doi.org/10.1016/j.compscitech.2014.10.009

Tian, X., Hou, Z., Li, D., & Lu, B. (2016). 3D printing of continuous fiber reinforced composites with a robotic system for potential space applications.

Yakovlev, A., Trunova, E., Grevey, D., Pilloz, M., & Smurov, I. (2005). Laser-assisted direct manufacturing of functionally graded 3D objects. *Surface and Coatings Technology*, *190*(1), 15–24. https://doi.org/10.1016/j.surfcoat.2004.07.070

Yang, C., Tian, X., Liu, T., Cao, Y., & Li, D. (2017). 3D printing for continuous fiber reinforced thermoplastic composites: mechanism and performance. *Rapid Prototyping Journal*, *23*(1), 209–215. https://doi.org/10.1108/RPJ-08-2015-0098

Zhong, W., Li, F., Zhang, Z., Song, L., & Li, Z. (2001). Short fiber reinforced composites for fused deposition modeling. *Materials Science and Engineering A301*, *301*, 125–130. https://doi.org/10.1016/S0921-5093(00)01810-4

Ziemian, S., Okwara, M., & Ziemian, C. W. (2015). Tensile and fatigue behavior of layered acrylonitrile butadiene styrene. *Rapid Prototyping Journal*, *21*(3), 270–278. https://doi.org/10.1108/RPJ-09-2013-0086